



## Influence of Annealing Temperature on the Phase Transformations of Composite Electroless Ni-P-X, X=SiC, Al<sub>2</sub>O<sub>3</sub> Coatings

R. González-Parra\*<sup>1</sup> • A. Bolarín-Miró<sup>2</sup> • F. Sánchez-de Jesús<sup>2</sup> • R. Valdez-Navarro<sup>1</sup>  
G. Agredo-Díaz<sup>3</sup> • N. Ortiz-Godoy<sup>3</sup> • C. Cruz<sup>4</sup> • A. Barba-Pingarrón<sup>1</sup>

<sup>1</sup>Centro de Ingeniería de Superficies y Acabados (CENISA). Facultad de Ingeniería UNAM. Circuito Exterior Ciudad Universitaria, Cdmx.

<sup>2</sup>Área Académica de Ciencias de la Tierra y Materiales. Universidad Autónoma del Estado de Hidalgo. Pachuca, Hidalgo, México.

<sup>3</sup>Departamento de Ingeniería Mecánica y Mecatrónica. Universidad Nacional de Colombia, Sede Bogotá. Ciudad Universitaria. Bogotá, Colombia

<sup>4</sup>Centro de Ingeniería y Desarrollo Industrial (CIDESI) Unidad Querétaro.

Received: 12 21 2023; Accepted: 09 24 2025

Available: 12 31 2025

**Abstract:** This paper presents a characterization of the phase transformations observed in a series of electroless Ni-P coatings on aluminum containing 2 wt. % of SiC or Al<sub>2</sub>O<sub>3</sub> particles and heat treated at 300 or 400°C for an hour. The composite electroless nickel coatings obtained were characterized using optical microscopy, scanning electron microscopy, microanalysis, interferometric microscopy, microhardness tests, roughness evaluation, and X-ray diffraction. The results indicate that the presence of the particles leads to a slight increase in the microhardness and the roughness of the deposits. Additionally, the coatings undergo crystallization and generate nickel phosphide (Ni<sub>3</sub>P) upon heat treatment at 400°C for 1 hour. A precipitation hardening mechanism significantly increases the microhardness of the coatings.

**Keywords:** Composite electroless nickel coatings, phase transformations, heat treating, microhardness.

\*Corresponding author.

E-mail address: [jesus.gonzalez@ingenieria.unam.edu](mailto:jesus.gonzalez@ingenieria.unam.edu) (R. González-Parra).

Peer Review under the responsibility of Universidad Nacional Autónoma de México.

## 1. Introduction

Since its discovery in the 1940s, electroless nickel plating processes have undergone significant development and are now widely used due to their particular and advantageous features (Chintada et al., 2021; Chintada et al., 2023; Nazari et al., 2023). This process involves the autocatalytic chemical reduction of nickel ions ( $\text{Ni}^{+2}$ ) present in a solution of nickel salts. A substance that acts as a reducer, such as sodium hypophosphite, (although boron-based compounds have also been used for this purpose (Nemane et al., 2024), without the use of any electric current in an acidic bath (Barba et al., 2021). The coatings formed using sodium hypophosphite as a reducing agent are typically Ni-P alloys, with a weight percentage of 3-18% (Yan et al., 2008).

The properties of these coatings depend on the phosphorus content of the coatings and the pH of the solution used. One of the main qualities of this

type of coating is the homogeneity in the thickness of the deposits, which remains almost constant regardless of the geometry of the substrate. Additionally, the autocatalytic condition of the process is a positive feature. Electroless nickel coatings can be obtained on a variety of metallic materials with different degrees of difficulty. Also, it is possible to obtain these coatings on certain polymeric and ceramic materials, although the preparation process is more complex.

The hardness of the deposits generally decreases with increasing phosphorus content. However, this increase improves the coatings' corrosion resistance (Barba et al., 2021; Yan et al., 2008). It is also worth noting that heat treatments can be applied to the coatings. Low-temperature heat treatments (around 200 to 300°C) have been shown to have minimal impact on coating properties, as documented by various authors, including Keong et al. (2003), Shetty et al. (2021), Guo et al. (2003), Ahmadkhaniha et al. (2021) and Palaniappa et al. (2007). It is important to maintain objectivity in reporting these findings. According to Balaraju et al. (2006) and Biswas et al. (2022), heat treatment at 400°C for 1 hour is the optimal temperature and time for inducing favorable changes in the microhardness of high-phosphorus coatings (8-9 wt.% P).

The crystallization process improves the mechanical properties of the coatings but also reduces their corrosion resistance. The original amorphous coatings had excellent corrosion resistance, especially in acidic environments (Pacheco et al., 2008; Azadi et al., 2021; Shozib et al., 2022). Some variants of electroless nickel coatings

involve adding a third element, Ni-P-(X), such as Mo, W, Cu, Zn, Sn, and Re. These modifications can improve wear and corrosion resistance, depending on the element and amount added to the electroless nickel plating bath. However, the addition of a third element can cause a less stable bath and a lower deposition rate (Mendoza et al., 2006; Palaniappa et al., 2007; Shahzad et al., 2020; Biswas et al., 2022).

Another widely applied modification is composite electroless nickel coatings. These coatings consist of hard ceramic particles (such as SiC,  $\text{Al}_2\text{O}_3$ ,  $\text{Si}_3\text{N}_4$ , diamond, WC,  $\text{TiO}_2$ , BN,  $\text{B}_4\text{C}$ ,  $\text{SiO}_2$ , and others) and soft particles with lubricating qualities (such as Teflon or molybdenum disulfide) that are added to the bath. These studies suggest that the addition of certain elements can enhance the wear resistance of the coatings without compromising their corrosion resistance (Agarwala et al., 2003; Balaraju et al., 2006; Sudagar et al., 2019; Nazari et al., 2023).

Regarding Ni-P- $\text{Al}_2\text{O}_3$  coatings, a consensus is reported that the addition of aluminum oxide particles effectively improves the wear resistance of the deposits. (Alirezai et al., 2007; León-Patiño et al., 2019; Hu et al., 2018). Alirezai et al. (2004) pointed out that, depending on the amount of added particles, their presence influences the deposition speed, roughness, and microhardness; the latter will increase in relation to the increase in the amount of alumina particles added.

In a subsequent study, Alirezai et al. (2007) investigated the wear resistance of electroless nickel-plated carbon steel with added aluminum oxide particles using a pin-on-disc wear test. The researchers found that the wear resistance was significantly improved when the Ni-P- $\text{Al}_2\text{O}_3$  coatings were heat-treated at 400°C for one hour, primarily due to the presence of  $\text{Ni}_3\text{P}$ . Similarly, it has been reported that the hardness decreases after treatment at 600°C, which appears to be associated with the growth of  $\text{Ni}_3\text{P}$  precipitates.

Hu et al. (2018) reported that the addition of  $\text{Al}_2\text{O}_3$  nanoparticles to an electroless Ni-P coating on magnesium alloys can increase microhardness and corrosion resistance by controlling the coating layer's grain size, without altering coating adhesion. León-Patiño et al., (2019) found that the wear rate of Ni-P- $\text{Al}_2\text{O}_3$  coatings decreases by one order of magnitude compared to electroless Ni-P coatings when tested under different conditions using a linear reciprocating wear test configuration. This test indicates the presence of both adhesive and abrasive wear mechanisms. For a more comprehensive review of the effect of incorporating nanoparticles into electroless nickel coatings, refer to Nazari et al. (2023).

The addition of SiC particles to coatings results in a slight increase in roughness and microhardness, as reported by Apachitei et al. (2002), Chang et al. (2016), Franco et al. (2013), Grosjean et al. (2001), and Soleimani et al. (2015). However, the increase in microhardness depends on the SiC content, and there is a limit beyond which no further beneficial effect on microhardness occurs (Franco et al., 2013).

Regarding the effect of the application of heat treatments, there is an agreement in the literature that the treatment at 400°C for 1 hour produces the best results in relation to the increase in microhardness and wear resistance (Shetty et al., 2021; Apachitei et al., 2002; Changet al., 2016; Franco et al., 2013; Vojtěch, 2009). At higher thermal treatments (500°C), a decrease in wear resistance is observed, attributed to the coarsening of Ni<sub>3</sub>P precipitates.

On the other hand, the addition of small amounts of SiC to Ni-P-(X) coatings does not significantly alter their corrosion resistance. Some studies have investigated the relationship between particle size and corrosion resistance, suggesting that nanometric-sized particles can enhance the corrosion resistance of deposits (Soleimani et al., 2015; Chintada et al., 2018). Additionally, it has been found that there is an optimal nanometric size that can achieve greater benefits in corrosion resistance (Farzaneh et al., 2016).

However, further research is needed to fully understand the relationship between corrosion resistance in various media and the addition of SiC particles to electroless Ni-P coatings, as the results are not yet conclusive (Zhang et al., 2008). According to Ahmadkhanha et al. (2018), the anodic polarization behavior of the coatings changed from passive to active after heat treatment at 400°C for 1 hour, compared with the as-plated condition. However, there is a lack of conclusive evidence on this point despite extensive research by several groups.

Information on the phase transformations in Ni-P-(X) coatings and their impact on mechanical and corrosion behavior remains insufficient. This study reports the characterization of Ni-P-(Al<sub>2</sub>O<sub>3</sub>;SiC) composite coatings on aluminum. Scanning electron microscopy, interferometric microscopy, microanalysis, microhardness, and X-ray diffraction were used to investigate the influence of phase transformations on the coatings.

## 2. Materials and Methods

The coatings were applied on commercially pure aluminum sheets, with a square section of 1 cm<sup>2</sup>. The specimens were initially washed with soap and water,

rinsed in running water, and immersed in a 5% NaOH solution at 40 °C for 90 seconds. After another rinse, the pieces were placed in a 1:1 solution of HNO<sub>3</sub> and ammonium fluoride at room temperature for 2 minutes, then rinsed. Subsequently, the samples were immersed in a solution containing 15 g/l of zinc oxide, 300 g/l of sodium hydroxide, 3 g/l of ferric chloride, 1.5 g/l of salicylic acid, and 8 g/l of sodium gluconate, for 45 seconds in each bath at room temperature. Later, rinse at the end of this bath sequence.

Electroless nickel plating was performed (Barba et al, 2021) with the addition of 2% by weight of aluminum oxide particles (1 μm, diameter) or 2% by weight of silicon carbide particles (1-5 μm size) using a pH of 4.6-4.7, measured with a pH-meter, Metrohm brand, model 620. The pH was adjusted by adding ammonia, and the bath temperature was maintained at 80-85°C for 90 and 120 minutes. A magnetic stirrer was set to 60 rpm.

Some of the samples were thermally treated in a muffle-type electric resistance furnace, Brand Hobersal, Model JB-20. The heat treatment cycles applied were 300 °C for 1 hour and 400 °C for 1 hour, with subsequent air cooling. The thickness was evaluated according to ASTM B487-20 (ASTM, 2020), in which the samples were cut into cross-sections, prepared metallographically by sanding with silicon carbide sandpaper up to grade 1000, and polished with 5- and 1-micrometer diamond pastes. For microscopic observation, an optical microscope (Epivert Leitz) and a scanning electron microscope (model Stereoscan 360, Leica) were used.

An interferometric microscope Zygo, model NewView100, was used to obtain the variations of the roughness of the surface coatings using a 40X objective. To perform microanalysis, a Cameca brand microprobe, model SX50, was used. We worked with LiF analyzer crystals, a voltage of 20kV, an output angle of 40°, an acquisition time of 30 seconds, and a current intensity of 20nA. For each sample analyzed, measurements were made at 5 to 7 different points on the coatings.

To obtain the hardness, an Akashi model MVK-HO microhardness tester was used, following the ASTM B-578-21 (ASTM, 2021) standard, using loads of 25 grams for the thinner layers and 100 grams for the rest of the coatings, applying the load for 15 seconds in 10 to 15 different sites for each of the deposits. These measurements were taken in the cross-section to avoid the influence of substrate hardness.

For the X-Ray Diffraction studies, a Siemens Model D-500 Diffractometer was used with Brentano Bragg Geometry  $\theta/2\theta$ , using Cu K $\alpha$  radiation ( $\lambda=1.5418$  Angstroms)

at 30 mA and 40kV, performing sweeps from 10 to 100°, with a step size of 0.05° and a time between steps of 3 seconds.

### 3. Results and Discussion

Figure 1 displays an optical microscopy image of an electroless nickel coating Ni-P-2%SiC composite. The image shows a uniform thickness and distribution of silicon carbide particles. Figure 2 presents an electron micrograph of the same type of deposit after heat treatment at 400°C for 1 hour. Morphologically, no significant differences are observed between the two images. The coating thickness ranged from 15 to 30 micrometers. The achieved thickness remained uniform regardless of the substrate geometry, and the presence of particles did not significantly alter the thickness. The chemical composition, obtained through electron microprobe analysis, revealed that the Ni-P, Ni-P-SiC, and Ni-P-Al<sub>2</sub>O<sub>3</sub> electroless coatings contained between 86.7% and 88.13% by weight of Ni and 11.87% and 13.24% by weight of P, resulting in high-phosphorus coatings.

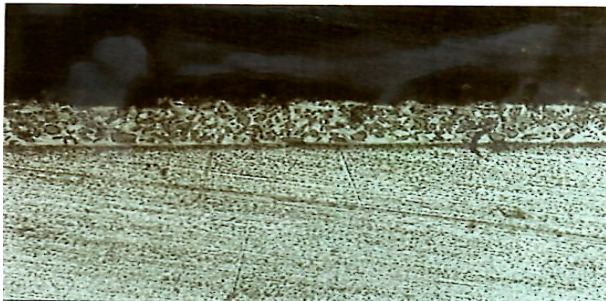


Figure 1. Composite electroless Ni-P-2%SiC coating on Al without heat treatment. OM, 260X.

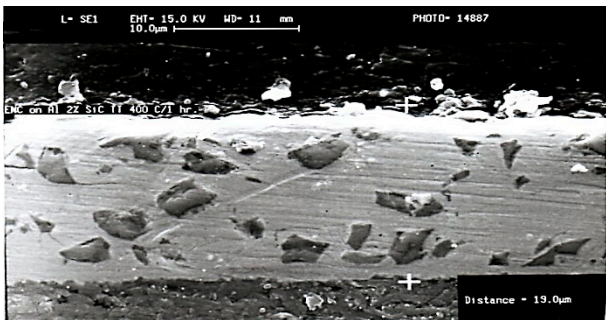


Figure 2. SEM Image of an Electroless Ni-P- 2%SiC, after heat treatment, 400°C/1 hour. 2500 X.

Figure 3 shows an optical microscopy image of an electroless nickel coating containing 2% Al<sub>2</sub>O<sub>3</sub>. The particles

are distinguishable when compared to the SiC particles in Figure 4. The coating morphology varies with the addition of different types of particles. The addition of SiC particles does not significantly alter the morphology, whereas alumina particles tend to agglomerate, altering the coating's roughness.

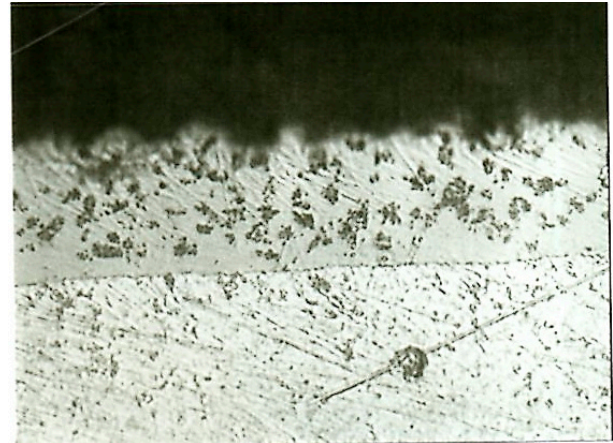


Figure 3. Composite Electroless Ni-P-2%Al<sub>2</sub>O<sub>3</sub>, without heat treatment. OM. 650X.

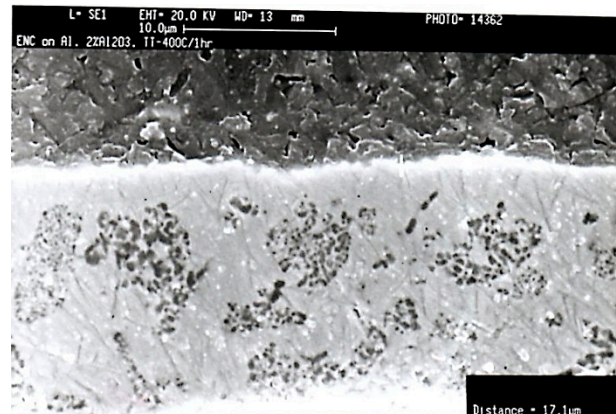


Figure 4. SEM image of a composite electroless Ni-P- 2%Al<sub>2</sub>O<sub>3</sub>, after heat treatment 400°C/1 hour. SEM. 3000X.

Figure 5 shows the impact of heat treatment (400°C/1 hour) on the microhardness of composite electroless nickel coatings. The microhardness of the coatings reached 1000 Vickers when aluminum oxide particles were added and 1100 Vickers when silicon carbide particles were added. This is slightly higher than the microhardness of Ni-P-Al<sub>2</sub>O<sub>3</sub> deposits, which may be due to silicon carbide's higher hardness than aluminum oxide.

Figure 6 (a) shows the diffractogram corresponding to an electroless nickel coating, in which the amorphous

condition of the coating and the identification of crystalline Al (reference 00-004-0787) and Ni (Reference 01-088-2326) are evident. When the deposit is subjected to heat treatment at 400°C/1 hour (Figure 6 (b), Ni appears crystalline, and the nickel phosphide Ni<sub>3</sub>P (JPCD 34-0501) was formed.

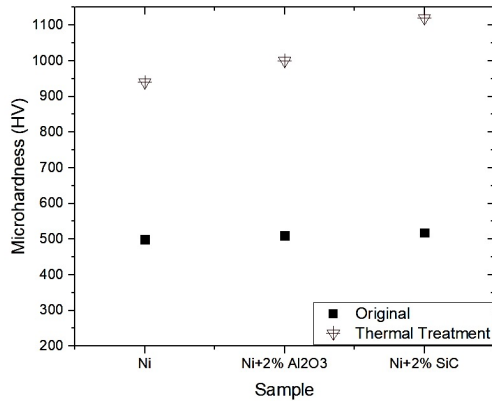
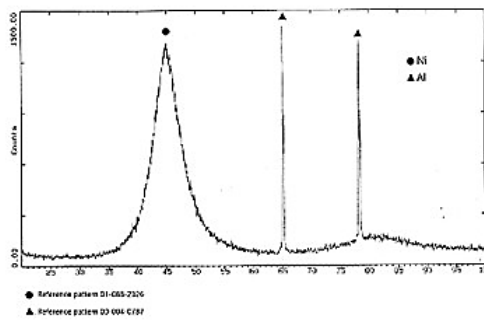
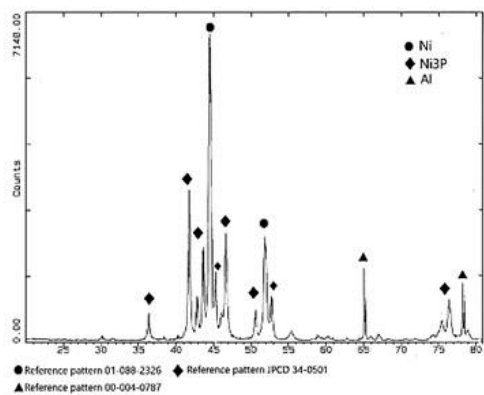


Figure 5. Effect of heat treatment (400°C/1 hour) on microhardness of composite electroless Ni-P-2%Al<sub>2</sub>O<sub>3</sub> and Ni-P-2%SiC coatings.



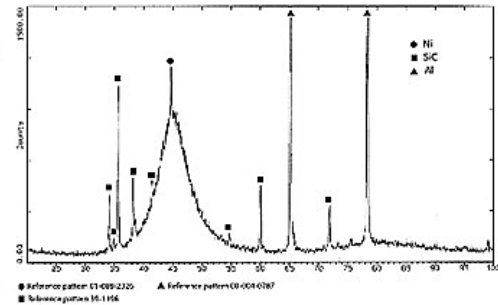
(a)



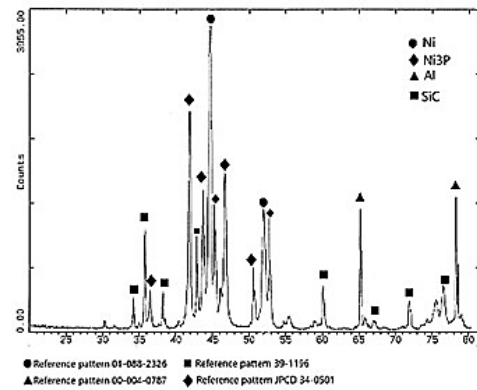
(b)

Figure 6. (a) Diffractogram of a Ni-P electroless nickel deposit, without heat treatment. (b) Diffractogram of a Ni-P electroless nickel coating after 400°C/1 hour heat treatment.

Similarly, Figure 7 (a) shows the recently deposited Ni-P-2%SiC electroless nickel coating composite, where the presence of Ni, Al, and SiC (JPCD reference 39-1196) is identified, while in Figure 7(b) the coating can be seen after having applied a heat treatment at 400°C for 1 hour. The effect of the heat treatment is reflected in the appearance of the crystalline Ni, nickel phosphide Ni<sub>3</sub>P, and SiC.



(a)

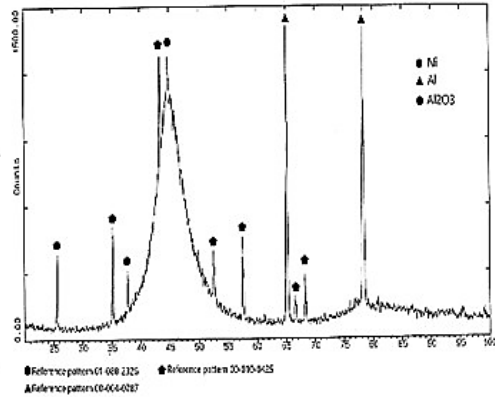


(b)

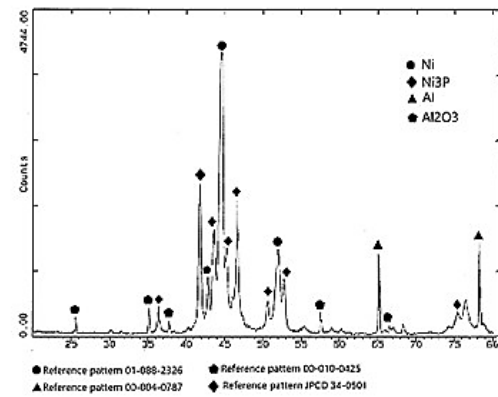
Figure 7. (a) Diffractogram of a Ni-P-2%SiC composite electroless nickel deposit, without heat treatment; (b) Diffractogram of a Ni-P-2%SiC composite electroless nickel coating after 400°C/1 hour heat treatment.

Figure 8(a) displays the diffractogram of a composite electroless nickel coating containing Ni, Al, and Al<sub>2</sub>O<sub>3</sub> (JPCD reference 00-010-0425). Figure 8(b) shows the coating after heat treatment at 300°C for 1 hour, revealing the crystalline phases Ni, nickel phosphide (Ni<sub>3</sub>P), and Al<sub>2</sub>O<sub>3</sub>.

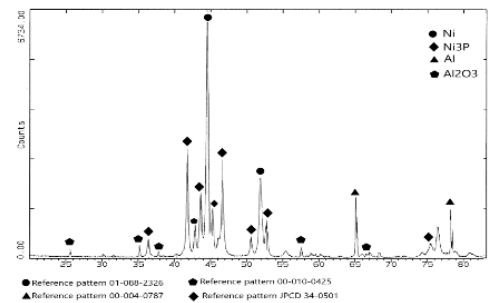
The heat treatment has a noticeable effect on the coating's appearance. Figure 8 and Table 1 show that the X-ray diffraction peak intensities of the coated samples heat-treated at 400°C are higher than those reported at 300°C. This suggests an incomplete transformation at 300°C, which is completed at 400°C (Keong et al., 2003; Shetty et al., 2021; Palaniappa et al., 2007; Franco et al., 2013; Biswas et al., 2016).



(a)



(b)



(c)

Figure 8 (a). Diffractogram of a Ni-P-2%Al<sub>2</sub>O<sub>3</sub> composite electroless nickel deposit, without heat treatment; (b) Diffractogram of a Ni-P-2%Al<sub>2</sub>O<sub>3</sub> composite electroless nickel coating after 300°C/1 hour heat treatment; (c) Diffractogram of a Ni-P-2%Al<sub>2</sub>O<sub>3</sub> composite electroless nickel coating after 400°C/1 hour heat treatment.

The increase in microhardness of the coatings is primarily due to the complete crystallization of Ni at 400°C, which was initially amorphous in deposits with high P, and to the formation of the Ni<sub>3</sub>P nickel phosphide precipitate. At lower heat treatment temperatures (300°C), the process of nickel crystal formation has not been completed, resulting in coatings containing micro or nanocrystalline Ni and another amorphous part of Ni.

Table 1. Maximum peaks of X Ray Diffraction of composite electroless Ni-P-X (Al<sub>2</sub>O<sub>3</sub>, SiC) with and without heat treatment.

Sample	Coating Characteristics and H.T	CPS (Max) Ni	CPS (Max) Ni <sub>3</sub> P
1	Ni-P without particles, 300°C/1 hour	5120	2596
2	Ni-P-2%Al <sub>2</sub> O <sub>3</sub> , 300°C/1 hour	2588	2228
3	Ni-P-2%SiC, 300°C/1 hour	3559	2220
4	Ni-P without particles, 400°C/1 hour	7148	3374
5	Ni-P-2%Al <sub>2</sub> O <sub>3</sub> , 400°C/1 hour.	6682	2920
6	Ni-P-2%SiC, 400°C/1 hour	3695	2702

Higher heat-treatment temperatures (500°C) cause precipitate particles to grow beyond the optimum size, resulting in a decrease in microhardness (Ahmadkhaniha et al., 2018). In Ni-P-SiC deposits, heat treatment at 500°C leads to the formation of NiSi<sub>2</sub> compounds, which degrade their tribological properties (Apachitei et al., 2002; Franco et al., 2013; Chang et al., 2016).

Table 2 displays the roughness values obtained by interferometric microscopy. It is evident that the value of Ra increases as particles are added. Alumina particles have a spherical morphology, while SiC particles have an acicular and irregular morphology. This difference is reflected in the higher roughness of SiC, which is expected to affect the coatings' behavior under wear conditions.

Table 2. Roughness of the composite electroless nickel coatings obtained under different heat treatment conditions, evaluated by interferometric microscopy.

Electroless Nickel Coating	Roughness, Ra (microns)
Ni-P without particles, No Heat Treatment (H.T.).	0.321
Ni-P-2%Al <sub>2</sub> O <sub>3</sub> , without H.T.	1.542
Ni-P-2% Al <sub>2</sub> O <sub>3</sub> , 300°C/1 hour	2.042
Ni-P-2% Al <sub>2</sub> O <sub>3</sub> , 400°C/1 hour	2.398
Ni-P-2%SiC, without H.T.	1.911
Ni-P-2%SiC, 300°C/1 hour	2.903
Ni-P-2%SiC, 400°C/1 hour	3.630

Figure 9 shows the morphology of a Ni-P-2%Al<sub>2</sub>O<sub>3</sub> composite electroless nickel, without heat treatment, obtained using interferometric microscopy, in which the presence of a “smooth” Ni-P matrix is clearly perceived and protruding.

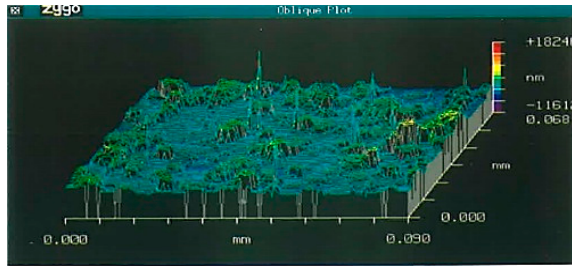


Figure 9. Roughness of a composite electroless Ni-P-2%Al<sub>2</sub>O<sub>3</sub>, without heat treatment. IM. 40X Ra average 1.542 μm.

Figure 10 shows an interferometric microscopy image of a Ni-P-2%SiC composite electroless nickel coating without heat treatment, in which the irregular (acicular) morphology of the SiC particles causing a greater roughness with respect to those of Al<sub>2</sub>O<sub>3</sub>.

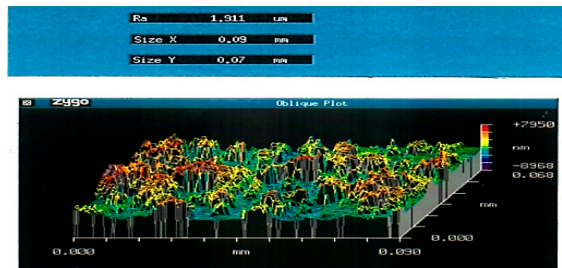


Figure 10. Interferometric microscopy image of Ni-P-2%SiC composite electroless nickel coatings, without heat treatment. “Ragged” morphology caused by the particles. ME. 40X Ra average 2.038 μm.

Figure 11 shows the joint effect of applying the heat treatment at 400°C for 1 hour and the presence of SiC particles. Heat treatment causes crystallization of the coating, leading to the formation of crystalline Ni and Ni<sub>3</sub>P, which explains the increase in roughness and should affect behaviors such as corrosion and wear resistance.

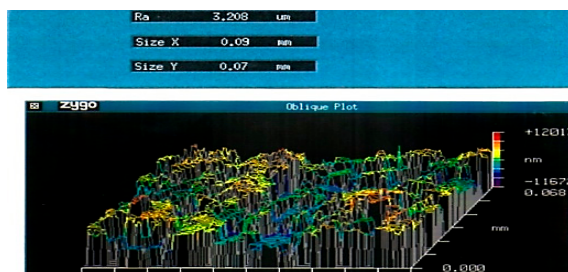


Figure 11. Roughness of a composite electroless Ni-P-2%SiC, after heat treatment 400°C, 1 hour. IM. 40X. Ra average: 3.630 μm.

Based on the literature and the findings of this paper, it is widely agreed that electroless Ni-P can exhibit various crystallographic conditions at the outset. At low or medium P levels, the coatings exhibit crystalline or microcrystalline structures (and even nanocrystalline structures, depending on the process conditions). However, at higher P levels (such as the 11-13% used in this research), the coatings tend to be predominantly amorphous. As a result, coatings with lower P levels exhibit greater microhardness.

According to the Ni-P phase diagram (Kim et al., 2014), the electroless Ni-high P coatings will undergo crystallization upon heating. The nickel, which was initially amorphous in the deposit, will crystallize, and Ni<sub>3</sub>P, nickel phosphide, will also form. This can be confirmed by examining the corresponding diffractograms before and after the heat treatment, particularly at 400 °C for 1 hour.

Another phenomenon that accompanies the previous one is the formation and precipitation of Ni<sub>3</sub>P from a supersaturated solution of P in Ni. Different researchers have found that the optimal point for the size and distribution of the precipitate, resulting in the most significant increase in coating microhardness, is achieved when heat-treated at 400°C for one hour (Keong et al., 2003; Palaniappa et al., 2007; Mendoza et al., 2006).

Based on the results obtained, it appears that the transition from the amorphous to the crystalline phase and the precipitation of the intermetallic phase (Ni<sub>3</sub>P) are temperature-dependent processes rather than heat-treatment time-dependent.

The addition of SiC and Al<sub>2</sub>O<sub>3</sub> particles initially increases roughness, which is expected to improve wear resistance subsequently. The extent of the effect depends mainly on the morphology of the particles and the amount added. According to Corredor et al. (2007), the roughness of Ni-P-SiC coatings is influenced not only by the shape of the particles (acicular for SiC and spherical for Al<sub>2</sub>O<sub>3</sub>) but also by the type of additives used. The interferometric microscopy images adequately reflect that the roughness of composite electroless nickel deposits increases when they are heat-treated (400°C/one hour) due to the crystallization of Ni and the formation of the Ni<sub>3</sub>P precipitate.

The influence of the added particles on microhardness modification is reduced in this work. The increase in microhardness of the coated samples after heat treatment at 400°C for one hour is mainly attributed to the crystallization of Ni and the formation of Ni<sub>3</sub>P precipitates in optimal quantity and distribution. At lower heat treatment temperatures, the composite electroless nickel coatings

exhibit some degree of stability, and the transformation is partial. At higher heat-treatment temperatures, agglomeration of the Ni<sub>3</sub>P precipitates reduces hardness.

Recently, hard nanoparticles have been used to develop composite electroless nickel coatings, offering new possibilities for improved properties and expanded applications. For instance, the addition of SiC nanoparticles (Chintada et al., 2018; Soleimani et al., 2015) has been reported to increase corrosion resistance. Similarly, the use of hard or soft nanoparticles (Nazari et al., 2023) can modify wear resistance and friction behavior.

## Conclusions

Composite electroless nickel coatings (Ni-P-SiC and Ni-P-Al<sub>2</sub>O<sub>3</sub>) were successfully produced on aluminum with uniform thickness and good adhesion.

The addition of 2% wt. SiC and Al<sub>2</sub>O<sub>3</sub> particles did not alter the amorphous structure of the coating but did increase its microhardness. However, it also led to increased coating roughness, as evaluated by interferometric microscopy.

Heat treatment at 300°C for 1 hour results in partial transformation of the deposits, producing a coating composed of amorphous nickel, crystalline nickel, and a portion of nickel phosphide (Ni<sub>3</sub>P).

Subsequent heat treatment at 400°C for 1 hour significantly modifies the coatings' properties, increasing microhardness from approximately 500 Vickers to just over 1100 Vickers. Heat treatment significantly increases the roughness of composite electroless nickel coatings.

The main mechanism responsible for this modification is the crystallization of the nickel in the coatings. Additionally, the process of precipitation hardening of Ni<sub>3</sub>P precipitates occurs, which is completed when treated at 400°C for one hour.

## Conflict of interest

The authors have no conflict of interest to declare.

## Funding

The authors received no specific funding for this work.

## Acknowledgements

This work was supported by Dirección General de Asuntos del Personal Académico – UNAM –PAPIIT IT100426

“Desarrollo de Tecnologías de Modificación Superficial para Aplicaciones Industriales, Aeroespaciales y Biomédicas”. Also, the authors acknowledge the Departamento de Ingeniería Química y Metalurgia – Universidad de Barcelona, Spain for the support provided during the experimental procedures.

## References

- Agarwala, R. C., & Agarwala, V. (2003). Electroless alloy/composite coatings: A review. *Sadhana*, 28(3), 475-493. <https://doi.org/10.1007/BF02706445>
- Ahmadkhaniha, D., Eriksson, F., Leisner, P., & Zanella, C. (2018). Effect of SiC particle size and heat-treatment on microhardness and corrosion resistance of NiP electrodeposited coatings. *Journal of Alloys and Compounds*, 769, 1080-1087. <https://doi.org/10.1016/j.jallcom.2018.08.013>
- Ahmadkhaniha, D., Lattanzi, L., Bonora, F., Fortini, A., Merlin, M., & Zanella, C. (2021). The effect of Co-Deposition of SiC sub-micron particles and heat treatment on wear behaviour of Ni-P coatings. *Coatings*, 11(2), 180. <https://doi.org/10.3390/coatings11020180>
- Alirezai, S., Monirvaghefi, S. M., Salehi, M. A. H. D. I., & Saatchi, A. (2004). Effect of alumina content on surface morphology and hardness of Ni-P-Al<sub>2</sub>O<sub>3</sub> (α) electroless composite coatings. *Surface and Coatings Technology*, 184(2-3), 170-175. <https://doi.org/10.1016/j.surfcoat.2003.11.013>
- Alirezai, S., Monirvaghefi, S. M., Salehi, M., & Saatchi, A. (2007). Wear behavior of Ni-P and Ni-P-Al<sub>2</sub>O<sub>3</sub> electroless coatings. *Wear*, 262(7-8), 978-985. <https://doi.org/10.1016/j.wear.2006.10.013>
- Apachitei, I., Tichelaar, F. D., Duszczuk, J., & Katgerman, L. (2002). The effect of heat treatment on the structure and abrasive wear resistance of autocatalytic NiP and NiP-SiC coatings. *Surface and Coatings Technology*, 149(2-3), 263-278. [https://doi.org/10.1016/S0257-8972\(01\)01492-X](https://doi.org/10.1016/S0257-8972(01)01492-X)
- ASTM B487-20, Standard Test Method for Measurement of Metal and Oxide Coating Thickness by Microscopical Examination of Cross Section.
- ASTM B578-2021, Standard Test Method for Microhardness of Electroplated Coatings.
- Azadi, M., Tavakoli, H., Haghghatkah, S., & Eranegh, F. A. (2021). Electrochemical Characteristics of Various Ni-P

- Composite Coatings in 0.6 M NaCl Solution. *Transactions of the Indian Institute of Metals*, 74(1), 137-147.  
<https://doi.org/10.1007/s12666-020-02125-1>
- Balaraju, J. N., Narayanan, T. S., & Seshadri, S. K. (2006). Structure and phase transformation behaviour of electroless Ni-P composite coatings. *Materials Research Bulletin*, 41(4), 847-860.  
<https://doi.org/10.1016/j.materresbull.2005.09.024>
- Barba, P.A. et al. (2021), "Niquelado químico", in Texto Iberoamericano de Ingeniería de Superficies, Mexico City, Mexico: *Facultad de Ingeniería UNAM*.
- Biswas, A., Das, S. K., & Sahoo, P. (2016). Effect of heat treatment duration on tribological behavior of electroless Ni-(high) P coatings. In *IOP Conference Series: Materials Science and Engineering* (Vol. 149, No. 1, p. 012045). IOP Publishing.  
<https://doi.org/10.1088/1757-899X/149/1/012045>
- Biswas, P., Das, S. K., & Sahoo, P. (2022). Evaluation of microhardness, wear, and corrosion behavior of duplex Ni-P/Ni-WP coatings. *Biointerface Res. Appl. Chem.*, 13(5), 416.  
<https://doi.org/10.33263/BRIAC135.416>
- Chang, C. S., Hou, K. H., Ger, M. D., Chung, C. K., & Lin, J. F. (2016). Effects of annealing temperature on microstructure, surface roughness, mechanical and tribological properties of Ni-P and Ni-P/SiC films. *Surface and Coatings Technology*, 288, 135-143.  
<https://doi.org/10.1016/j.surfcoat.2016.01.020>
- Chintada, V. B., & Koonan, R. (2018). Influence of SiC nano particles on microhardness and corrosion resistance of electroless Ni-P coatings. *Journal of Bio-and Tribo-Corrosion*, 4(4), 68.  
<https://doi.org/10.1007/s40735-018-0186-4>
- Chintada, V. B., Gurugubelli, T. R., Tamtam, M. R., & Koutavarapu, R. (2023). Advancements in nickel-phosphate/boron based electroless composite coatings: a comprehensive review of mechanical properties and recent developments. *Materials*, 16(18), 6116.  
<https://doi.org/10.3390/ma16186116>
- Chintada, V. B., Koonan, R., & Raju Bahubalendruni, M. V. A. (2021). State of art review on nickel-based electroless coatings and materials. *Journal of Bio-and Tribo-Corrosion*, 7(4), 134.  
<https://doi.org/10.1007/s40735-021-00568-7>
- Corredor Acuña, J., & Echeverría Echeverría, F. (2007). Deposición electroless de recubrimientos Ni-P y estudio de la influencia del contenido de fósforo en la resistencia a la corrosión. *Revista Facultad de Ingeniería Universidad de Antioquia*, (42), 57-67.
- Farzaneh, A., Ehteshamzadeh, M., Can, M., Mermer, O., & Okur, S. (2016). Effects of SiC particles size on electrochemical properties of electroless Ni-P-SiC nanocomposite coatings. *Protection of Metals and Physical Chemistry of Surfaces*, 52(4), 632-636.  
<https://doi.org/10.1134/S2070205116040109>
- Franco, M., Sha, W., Malinov, S., & Rajendran, R. (2013). Phase composition, microstructure and microhardness of electroless nickel composite coating co-deposited with SiC on cast aluminium LM24 alloy substrate. *Surface and Coatings Technology*, 235, 755-763.  
<https://doi.org/10.1016/j.surfcoat.2013.08.063>
- Grosjean, A., Rezzazi, M., Takadoum, J., & Bercot, P. (2001). Hardness, friction and wear characteristics of nickel-SiC electroless composite deposits. *Surface and Coatings Technology*, 137(1), 92-96.  
[https://doi.org/10.1016/S0257-8972\(00\)01088-4](https://doi.org/10.1016/S0257-8972(00)01088-4)
- Guo, Z., Keong, K. G., & Sha, W. (2003). Crystallisation and phase transformation behaviour of electroless nickel phosphorus platings during continuous heating. *Journal of Alloys and Compounds*, 358(1-2), 112-119.  
[https://doi.org/10.1016/S0925-8388\(03\)00069-0](https://doi.org/10.1016/S0925-8388(03)00069-0)
- Hu, R., Su, Y., Liu, Y., Liu, H., Chen, Y., Cao, C., & Ni, H. (2018). Deposition process and properties of electroless Ni-P-Al<sub>2</sub>O<sub>3</sub> composite coatings on magnesium alloy. *Nanoscale research letters*, 13(1), 198.  
<https://doi.org/10.1186/s11671-018-2608-0>
- Keong, K. G., Sha, W., & Malinov, S. (2003). Hardness evolution of electroless nickel-phosphorus deposits with thermal processing. *Surface and Coatings Technology*, 168(2-3), 263-274.  
[https://doi.org/10.1016/S0257-8972\(03\)00209-3](https://doi.org/10.1016/S0257-8972(03)00209-3)
- Kim, T. Y., Son, H. J., Lim, S. K., Song, Y. I., Park, H. S., & Suh, S. J. (2014). Electroless nickel alloy deposition on SiO<sub>2</sub> for application as a diffusion barrier and seed layer in 3D copper interconnect technology. *Journal of nanoscience and nanotechnology*, 14(12), 9515-9524.  
<https://doi.org/10.1166/jnn.2014.10173>
- León-Patiño, C. A., García-Guerra, J., & Aguilar-Reyes, E. A. (2019). Tribological characterization of heat-treated Ni-P and Ni-P-Al<sub>2</sub>O<sub>3</sub> composite coatings by reciprocating sliding tests. *Wear*, 426, 330-340.  
<https://doi.org/10.1016/j.wear.2019.02.015>

- Mendoza, L. V., Barba, A., Bolarin, A., & Sanchez, F. (2006). Age hardening of Ni–P–Mo electroless deposit. *Surface engineering*, 22(1), 58-62.  
<https://doi.org/10.1179/174329406X84976>
- Nazari, H., Barati Darband, G., & Arefinia, R. (2023). A review on electroless Ni–P nanocomposite coatings: effect of hard, soft, and synergistic nanoparticles. *Journal of Materials Science*, 58(10), 4292-4358.  
<https://doi.org/10.1007/s10853-023-08281-1>
- Nemane, V., & Chatterjee, S. (2024). Effect of silicon carbide incorporation and heat treatment on tribological properties of electroless Ni–B–W alloy coating. *Materials Chemistry and Physics*, 311, 128500.  
<https://doi.org/10.1016/j.matchemphys.2023.128500>
- Pacheco, D., León, O., Liscano, S., & Gil, L. (2008). Influencia de la temperatura de tratamiento térmico sobre la velocidad de corrosión de recubrimientos autocatalíticos Ni-P. *Universidad, Ciencia y Tecnología*, 12(47), 65-72.
- Palaniappa, M., & Seshadri, S. K. (2007). Structural and phase transformation behaviour of electroless Ni–P and Ni–W–P deposits. *Materials Science and Engineering: A*, 460, 638-644.  
<https://doi.org/10.1016/j.msea.2007.01.134>
- Shahzad, K., Fayyad, E. M., Nawaz, M., Fayyaz, O., Shakoor, R. A., Hassan, M. K., ... & Abdullah, A. M. (2020). Corrosion and heat treatment study of electroless nip-ti nanocomposite coatings deposited on hsla steel. *Nanomaterials*, 10(10), 1932.  
<https://doi.org/10.3390/nano10101932>
- Shetty, A. D., Shivamurthy, B., Thimmappa, B. H. S., & Parmar, Y. (2021). Heat treatment and quenching effects on wear of electroless nickel–phosphorous plating. *Cogent Engineering*, 8(1), 1959009.  
<https://doi.org/10.1080/23311916.2021.1959009>
- Shozib, I. A., Ahmad, A., Abdul-Rani, A. M., Beheshti, M., & Aliyu, A. A. A. (2022). A review on the corrosion resistance of electroless Ni-P based composite coatings and electrochemical corrosion testing methods. *Corrosion Reviews*, 40(1), 1-37.  
<https://doi.org/10.1515/corrrev-2020-0091>
- Soleimani, R., Mahboubi, F., Kazemi, M., & Arman, S. Y. (2015). Corrosion and tribological behaviour of electroless Ni–P/nano-SiC composite coating on aluminium 6061. *Surface Engineering*, 31(9), 714-721.  
<https://doi.org/10.1179/1743294415Y.0000000012>
- Sudagar, J., Muraliraja, R., Tamilarasan, T.R., Udayakumar, S. and Selvakumar, A. (2019), “Electroless Composite Coatings”, in *Electroless Nickel Plating*, Boca Raton, USA: CRC Press, pp. 359-409.  
<http://doi.org/10.1201/9780429466274-9>
- Vojtěch, D. (2009). Properties of hard Ni–P–Al<sub>2</sub>O<sub>3</sub> and Ni–P–SiC coatings on Al-based casting alloys. *Materials and Manufacturing Processes*, 24(7-8), 754-757.  
<https://doi.org/10.1080/10426910902809784>
- Yan, M., Ying, H. G., & Ma, T. Y. (2008). Improved microhardness and wear resistance of the as-deposited electroless Ni–P coating. *Surface and Coatings Technology*, 202(24), 5909-5913.  
<https://doi.org/10.1016/j.surfcoat.2008.06.180>
- Zhang, S., Han, K., & Cheng, L. (2008). The effect of SiC particles added in electroless Ni–P plating solution on the properties of composite coatings. *Surface and Coatings Technology*, 202(12), 2807-2812.  
<https://doi.org/10.1016/j.surfcoat.2007.10.015>